NASA/TM—2020-220512

Enabling Dynamic Vehicle Analyses With Improved Atmospheric Attenuation Models in Glenn Research Center Communication Analysis Suite

Cory T. Vitez and Bryan W. Welch
Glenn Research Center, Cleveland, Ohio

April 2020

NASA STI Program . . . in Profile

Since its founding, NASA has been dedicated to the advancement of aeronautics and space science. The NASA Scientific and Technical Information (STI) Program plays a key part in helping NASA maintain this important role.

The NASA STI Program operates under the auspices of the Agency Chief Information Officer. It collects, organizes, provides for archiving, and disseminates NASA's STI. The NASA STI Program provides access to the NASA Technical Report Server—Registered (NTRS Reg) and NASA Technical Report Server—Public (NTRS) thus providing one of the largest collections of aeronautical and space science STI in the world. Results are published in both non-NASA channels and by NASA in the NASA STI Report Series, which includes the following report types:

- TECHNICAL PUBLICATION. Reports of completed research or a major significant phase of research that present the results of NASA programs and include extensive data or theoretical analysis. Includes compilations of significant scientific and technical data and information deemed to be of continuing reference value. NASA counter-part of peer-reviewed formal professional papers, but has less stringent limitations on manuscript length and extent of graphic presentations.

- TECHNICAL MEMORANDUM. Scientific and technical findings that are preliminary or of specialized interest, e.g., "quick-release" reports, working papers, and bibliographies that contain minimal annotation. Does not contain extensive analysis.

- CONTRACTOR REPORT. Scientific and technical findings by NASA-sponsored contractors and grantees.

- CONFERENCE PUBLICATION. Collected papers from scientific and technical conferences, symposia, seminars, or other meetings sponsored or co-sponsored by NASA.

- SPECIAL PUBLICATION. Scientific, technical, or historical information from NASA programs, projects, and missions, often concerned with subjects having substantial public interest.

- TECHNICAL TRANSLATION. English-language translations of foreign scientific and technical material pertinent to NASA's mission.

For more information about the NASA STI program, see the following:

- Access the NASA STI program home page at http://www.sti.nasa.gov

- E-mail your question to help@sti.nasa.gov

- Fax your question to the NASA STI Information Desk at 757-864-6500

- Telephone the NASA STI Information Desk at 757-864-9658

- Write to:
  NASA STI Program
  Mail Stop 148
  NASA Langley Research Center
  Hampton, VA 23681-2199

NASA/TM—2020-220512

Enabling Dynamic Vehicle Analyses With Improved Atmospheric Attenuation Models in Glenn Research Center Communication Analysis Suite

Cory T. Vitez and Bryan W. Welch
Glenn Research Center, Cleveland, Ohio

National Aeronautics and
Space Administration

Glenn Research Center
Cleveland, Ohio 44135

April 2020

This report contains preliminary findings, subject to revision as analysis proceeds.

Level of Review: This material has been technically reviewed by technical management.

Available from

NASA STI Program
Mail Stop 148
NASA Langley Research Center
Hampton, VA 23681-2199

National Technical Information Service
5285 Port Royal Road
Springfield, VA 22161
703-605-6000

This report is available in electronic form at http://www.sti.nasa.gov/ and http://ntrs.nasa.gov/

Enabling Dynamic Vehicle Analyses With Improved Atmospheric Attenuation Models in Glenn Research Center Communication Analysis Suite

Cory T. Vitez* and Bryan W. Welch
National Aeronautics and Space Administration
Glenn Research Center
Cleveland, Ohio 44135

Summary

To aid in meeting the NASA objective of returning humans to the Moon, the Glenn Research Center's Communication Analysis Suite was augmented with two distinct capabilities. The first capability added was the vehicle propagator. This allows the addition of dynamic aircraft and ground vehicles around any celestial body within the solar system during an analysis. This functionality interpolates the position and velocity of the vehicle relative to a celestial body at the time steps analyzed using the type of path and either a series of waypoints or a direction and duration of travel. The implications of this new capability include lunar rovers and/or drones, such as Dragonfly, where the vehicle propagator will analyze the communications architecture. The newly created vehicle propagator is now in use in communications studies for the 2024 lunar missions, simulating the movement of lunar rovers across the Moon's southern pole. The second capability added was the augmentation of the atmospheric attenuation model. The previous model did not have a uniform low-elevation attenuation model due to the trigonometric approximation for path length and the exponential nature of low-elevation scintillation. User-defined weather parameters were also added to the updated atmospheric attenuation model. The previous model solely used tabular data based upon the season and location of the transmitting antenna. Multiple simulations of the same configuration now return different results based on the differing weather parameters. Cognitive communications analysis efforts can use this second capability to generate neural network training data based on differing weather conditions at utilized ground stations, a critical step in allowing neural networks to learn how weather parameters impact communications performance.

Nomenclature

A	altitude above reference ellipsoid
a	angle between λ_i, φ_i, and A_i and λ_{i-1}, φ_{i-1}, and A_{i-1}
BCBF	body-centered body-fixed
D	length of slant path
d	distance traveled along bodies surface
ENU	East North Up
f	difference between λ_i and λ_{i-1} or φ_i and φ_{i-1}
H	distance from ground level to height of the atmosphere
H_0	distance from ground level to height of the transmitting antenna
i	index of t_{user} (indexing starts at 1)
i_{max}	max index (length) of t_{user}

*Summer Intern in Lewis' Educational and Research Collaborative Internship Program (LeRCIP) and undergraduate at Purdue University.

ITU	International Telecommunication Union
k	number of time steps since motion started
max	maximum
R_E	radius of Earth
s	ground speed
t_{master}	time step where analysis is done
t_{user}	user-defined time step where corresponding location or direction is given
$\hat{v}$	velocity unit vector
v	velocity vector
x	unit vector from center of body towards λ = 0°, φ = 0°, and A = 0 in BCBF coordinate system
y	unit vector from center of body towards λ = 90°, φ = 0°, and A = 0 in BCBF coordinate system
z	unit vector from center of body towards λ = 0°, φ = 90°, and A = 0 in BCBF coordinate system
λ	geodetic longitude
φ	geodetic latitude
ϑ	true course (radians off north)
θ	elevation angle

1.0 Introduction

The missions to the Moon in 2024 and beyond require specific communications networks, which are best determined through network analyses. High-fidelity analysis of surface elements requires knowing the location of the vehicle at any time step used when calculating performance. To minimize user input burden and increase the vehicle propagator flexibility, it calculates the precise location of a vehicle at each time step, and allows multiple different input methods, which describe the path a vehicle takes. The vehicle propagator also supports future expandability and use cases. It works with any type of ground, air, or underground vehicle around any celestial body within the solar system. Accuracy improvements, such as detailed terrain mapping, can easily be added to more precisely know the altitude of a vehicle, improving analysis results.

The vehicle propagator updates necessitated updates to the Earth's atmospheric attenuation model. The previous model provided analysis for an elevation angle of 5° or above. With the addition of communication between vehicles, a use case for vehicles operating with less than 5° elevation angle was created. Thus, the atmospheric attenuation model was adjusted and the calculations were expanded to support the smaller elevation angle analysis. In addition, the atmospheric attenuation model was generalized to support user-defined custom weather parameters. Previously, the Earth's atmospheric attenuation model used a tabular reference process based on the time of year and location of the ground station antenna to approximate parameters used in the attenuation calculation. The addition of custom weather parameters allows the user to more accurately define the weather parameters at the location of the transmitting antenna. This not only improves the accuracy of the atmospheric attenuation calculations, but it also enables the ability to create training data based on changing weather parameters.

2.0 Vehicle Propagator

The vehicle propagator is composed of two main modes and three submodes. The two main modes are Waypoint and Course modes. Waypoint mode has the user specify waypoints and the times that the vehicle will reach those waypoints. Specification of one of the three submodes will define the trajectory that the vehicle follows from waypoint to waypoint. The vehicle propagator is then responsible for interpolating between these waypoints along the defined trajectory. The other main mode is Course mode. In Course mode, the user specifies a starting location, a set of directions, and the corresponding duration to travel in each specified direction. Course mode works similarly to Waypoint mode, in the sense that the vehicle propagator interpolates along the specified course. However, it is for the duration traveled in a specified direction and not a specified number of waypoints.

The three submodes of the vehicle propagator are the types of trajectories that the vehicle is traveling along. The trajectories currently implemented include Euclidean, great circle, and rhumb line, all of which can be compared in Figure 1. Euclidean (orange), great circle (red), and rhumb line (blue) paths are illustrated connecting a series of three points. The Euclidean paths are the shortest path. While they often go through the surface of the planetary body, they are useful for aerial vehicles and will be fundamental to future terrain mapping. Great circle paths are geodesics. They are the shortest path between two points while being constrained to travel along the surface of an ellipsoidal celestial body. These paths are useful for rovers and their implementation has been generalized to include changes in altitude. Rhumb lines, or loxodromes, are the path of constant bearing between two points on an ellipsoid. Like great circles, these have also been generalized to account for changes in altitude.

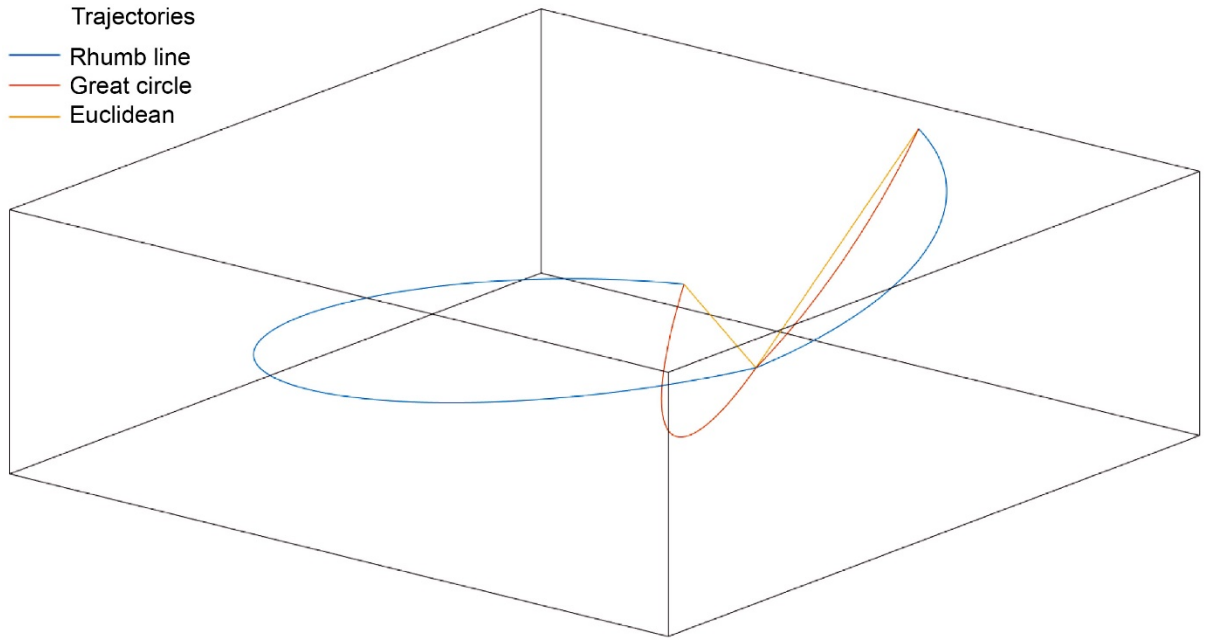

Figure 1.—Vehicle propagator trajectories supported.

2.1 Main Mode: Course

Course mode uses a user-defined series of bearings, the series of altitudes (A), the trajectory the vehicle is following (λ_1, φ_1, A_1, and $t_{user,1}$) and two of the following three parameters: distance (d), speed (s), and time. The time can either be in the format of t_{user}, which is a sequence of MATLAB® datetimes, or Δt_{user}, the duration of travel between two bearings. Course mode converts these parameters into λ, φ, and A at corresponding t_{user}, which are then used in the Waypoint mode function for interpolation.

$$\Delta t_{user} = \frac{d}{s} \tag{1}$$

$$t_{user,k} = t_{user,1} + \sum_{i=1}^{k-1} \Delta t_{user,i} \tag{2}$$

If Δt_{user} and t_{user} are both unknown, Δt_{user} is calculated using Equation (1). Then all the t_{user} values are calculated within a loop that uses a process similar to Equation (2), where k is the number of time steps since the motion started. If Δt_{user} or t_{user} are given, the other can be calculated through a variation of Equation (2). If d or s are unknown, they are calculated through Equation (1).

Once d, s, t_{user}, and Δt_{user} are known, they are passed into a subfunction based on the user-defined trajectory. Within that subfunction, λ and φ are calculated (Ref. 1) based on spherical geometries from the distance along the arc. The series of A is then appended and λ, φ, A, and t_{user} are passed into Waypoint mode to compute the interpolation. Course mode is illustrated in Figure 2. The green dot is the starting point, the yellow dot is the end point, the arrows show the bearing the user chose, the white lines represent the duration of travel along those bearings, and the pink dotted lines represent a trajectory for a longer duration.

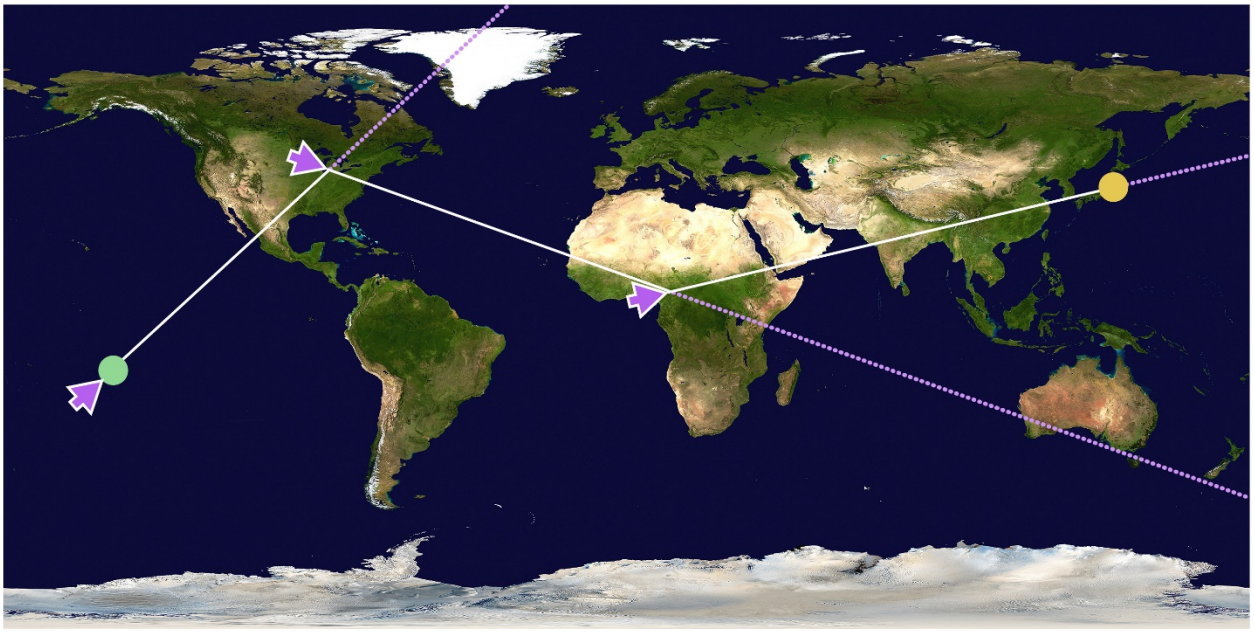

Figure 2.—Course mode interpolations.

It is important to note that many of these trajectory methods were defined along a perfect sphere. These trajectories were adopted to work on ellipsoids with changing A values. Gain or loss in A was taken as a separate component to φ and λ. Idealized spheres were utilized for the latitude and longitude components, while altitude variations were precompensated and postcompensated for the gain or loss in A. This prevents having great circle paths that were the same distance at different altitudes. This methodology futureproofs the capability for cases when the radius of the reference ellipsoid is not much larger than the altitude above the reference ellipsoid.

2.2 Main Mode: Waypoint

Waypoint mode is composed of a series of user-defined λ, φ, and A at corresponding t_{user}. The function loops over each t_{master} and finds the first $t_{\text{user,i}}$ after t_{master}. At the initial time step, the location of the vehicle is λ_1, φ_1, and A_1 and $\hat{v}$ is zero. Additionally, the vehicle propagator checks if $t_{\text{master}} \leq t_{\text{user,max}}$, where the location at every subsequent time step will be λ_i, φ_i, and A_i where $i = i_{\text{max}}$. The vehicle also knows that since the vehicle will no longer be moving, $\hat{v}$ will be zero for every time step subsequent to t_{master}.

Once the vehicle propagator checks that neither $i = 1$ nor $t_{\text{user}} \leq t_{\text{master}}$, the vehicle propagator checks if $\lambda_i = \lambda_{i-1}$ and $\varphi_i = \varphi_{i-1}$. If both of these conditions are met, the interpolation for A is a simple linear interpolation as seen in Equation (3) where Δt_{master} is the difference between the current t_{master} and the t_{master} directly before $t_{\text{master}} - 1$.

$$A_{t_{\text{master}}} = A_{i-1} + \Delta A \frac{\left(t_{\text{user},i} - t_{\text{master}}\right)}{\Delta t_{\text{master}}}$$
$$\Delta A = A_i - A_{i-1} \tag{3}$$

This condition does not need to be checked in Euclidean or rhumb line submodes, but when true, it reduces runtime by lowering the total number of computations to compute λ, φ, and A. Waypoint mode is illustrated in Figure 3. The green dots represent the waypoints that the user specifies and the white lines are the trajectories that the vehicle propagator will interpolate along, when calculating the vehicle's location at the specified times.

The vehicle propagator also checks if $t_{\text{master}} = t_{\text{user},i}$. In this case, λ_i, φ_i, and A_i is exactly the λ, φ, and A at t_{master}, however, $\hat{v}$ is undefined when $A_i = A_{i-1}$. If the velocity vector $\hat{v}$ happens to be undefined, the vehicle propagator arbitrarily uses $\hat{v}$ of the previous t_{master} in order to ensure $\hat{v}$ is always defined, as it is used within other parts of the communication analysis. If $A_i \neq A_{i-1}$, $\hat{v}$ is computed as the position difference against the time difference.

The vehicle propagator, lastly, interpolates along the trajectory the user defined. These calculations are further explained in Sections 3.3 to 2.5 along with the details of how the specific trajectories impact the above descriptions of the vehicle propagator. Figure 4 illustrates these three modes. Pictured are the three types of trajectories connecting two points. From left to right are great circles arcs, Euclidean straight lines, and rhumb line arcs.

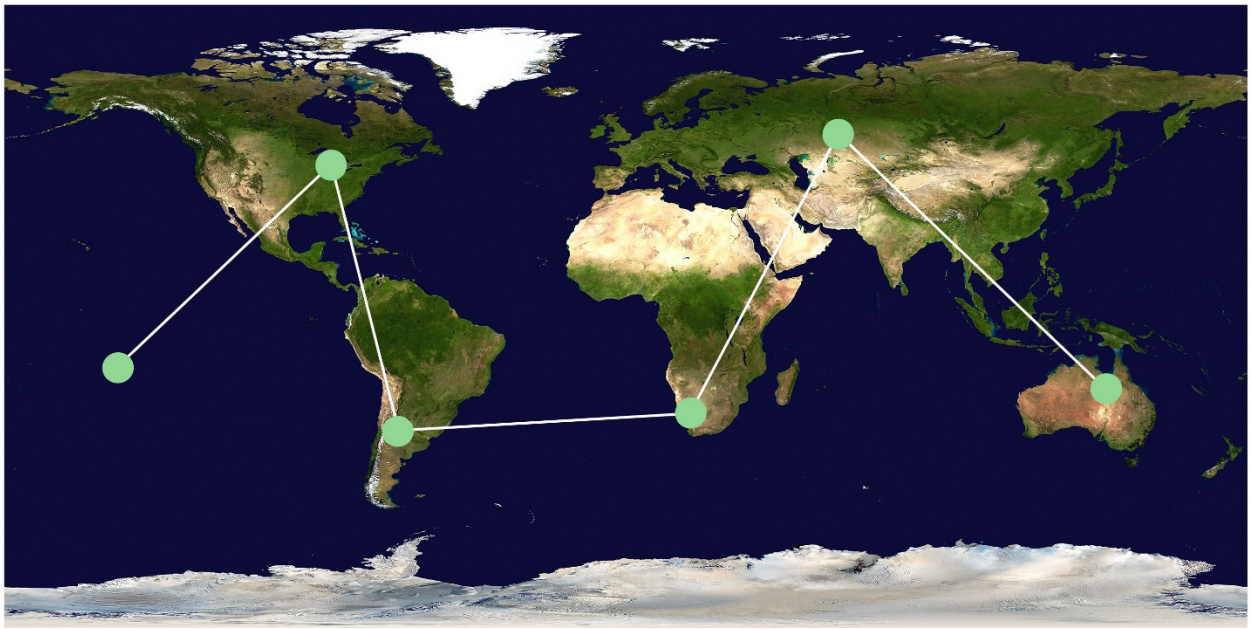

Figure 3.—Waypoint mode interpolations.

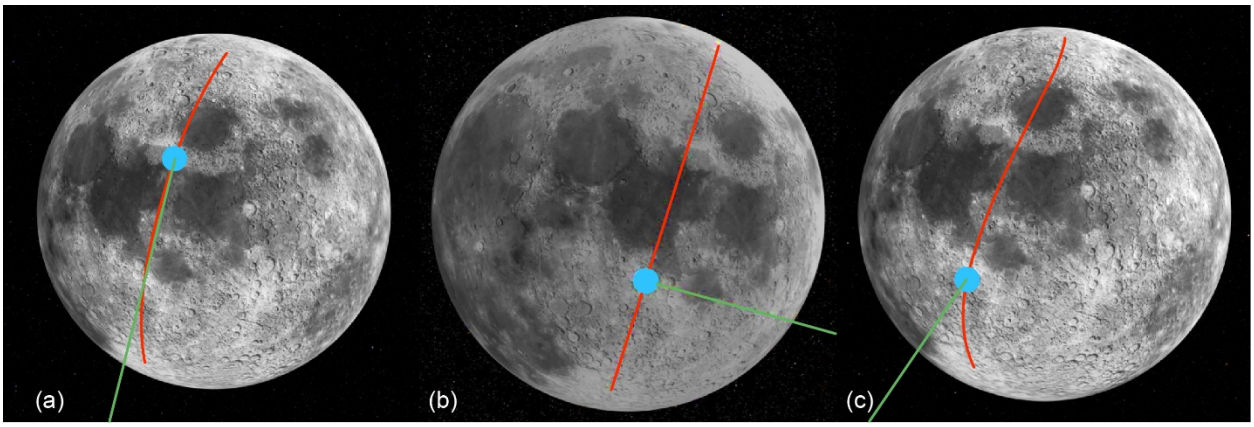

Figure 4.—Great circle, Euclidean, and rhumb line trajectories. (a) Great circle. (b) Euclidean. (c) Rhumb line.

2.3 Submode: Euclidean

The interpolation in Euclidean mode is a simple linear interpolation along the lines connecting the points λ_i, φ_i, and A_i and λ_{i-1}, φ_{i-1}, and A_{i-1}. Before this interpolation, the point λ, φ, and A are converted to body-centered body-fixed (BCBF) coordinates x, y, and z. A linear interpolation similar to Equation (3) uses an equation, which is used for each component individually; x, y, and z rather than A (i.e., x then y then z is substituted for A in Eq. (3)). Then, the s and $\hat{v}$ are then calculated from Equation (4).

$$v = \frac{\Delta x, \Delta y, \Delta z}{\Delta t_{\text{user}}} \qquad \hat{v} = \frac{v}{s} \qquad s = \|v\|$$
$$\Delta x = x_i - x_{i-1} \qquad \Delta y = y_i - y_{i-1} \qquad \Delta z = z_i - z_{i-1} \tag{4}$$

2.4 Submode: Rhumb Line

Rhumb line mode interpolation works similar to the Euclidean implementation. The approach uses Equation (3) for each position component λ, φ, and A where the components are substituted for A. Equation (3) works for rhumb lines because rhumb lines are lines of constant heading. This means, unlike with great circles, if you are a fraction, f, along a rhumb line, you would have traveled f difference between the λ_i and λ_{i-1} and f difference between φ_i and φ_{i-1}.

The rhumb line velocity is computed in a few steps. First, d is calculated (Ref. 1) the distance between the points λ_i, φ_i, and A_i and λ_{i-1}, φ_{i-1}, and A_{i-1}. Second, Δt_{user} and d are used in Equation (1) to compute s. Third, the direction of travel (true course ϑ) is computed (Ref. 1). The intermediate spherical coordinates are calculated using Equation (5). Using s and the direction of travel, the East North Up (ENU) velocity v_{ENU} is then calculated in the ENU reference frame using Equation (5). Finally, the ENU coordinates are transformed into BCBF coordinates (Ref. 2), finally calculating the BCBF velocity v_{BCBF}.

$$\lambda = \frac{d \sin \vartheta}{\Delta t_{\text{user}}} \qquad \varphi = \frac{d \cos \vartheta}{\Delta t_{\text{user}}} \qquad A = \frac{\Delta A}{\Delta t_{\text{user}}} \tag{5}$$

2.5 Submode: Great Circle

Great circle mode checks if the vehicle is traveling pole to pole, as great circles are undefined between endpoints at opposite poles of a body. If this is the case, the software algorithm uses the calculations from Rhumb line mode, which are defined as rhumb lines and great circles are the same trajectory when $\vartheta = 0$ or $\vartheta = \pi/2$.

In every other case, great circle mode calculates f, and the angle between λ_i, φ_i, and A_i and λ_{i-1}, φ_{i-1}, and A_{i-1}. Since the angle a between λ_i, φ_i, and A_i and λ_{i-1}, φ_{i-1}, and A_{i-1} is constant with constant velocity, the angle, a, between λ_{i-1}, φ_{i-1}, and A_{i-1} and the vehicle location is $f \cdot a$. Then, using circular geometry, λ, φ, and A are computed (Ref. 1) as they lie on the great circle made by λ_i, φ_i, and A_i and λ_{i-1}, φ_{i-1},and A_{i-1}, an angle $f \cdot a$ away from λ_{i-1}, φ_{i-1}, and A_{i-1} towards λ_i, φ_i, and A_i.

The algorithm computes velocity once the position is interpolated. The true course, ϑ, is calculated at the point λ, φ, and A that was just previously computed. The Δt_{user} and d are used in Equation (1) to compute s. The v_{ENU} is computed using Equation (5). Finally, the algorithm transforms v_{ENU} into v_{BCBF} (Ref. 2), becoming the vehicle's velocity at point λ, φ, and A.

3.0 Atmospheric Attenuation

The atmospheric attenuation model computes the loss between a ground asset on the Earth's surface with an asset in space. The previous algorithm limited the ground station's minimum elevation angle to 5°, consistent with the International Telecommunication Union (ITU) models between space and ground assets. To accommodate the surface vehicles, the minimum elevation angle was reduced to a half-degree to support communications links between vehicles. In order for these updates to become operational, two major changes were made. First, the slant path angle within the atmospheric rain loss function was updated to allow elevation angles below 5°. Second, the scintillation model was transformed into a uniform scintillation model for elevation angles less than 5°, to calculate atmospheric scintillation more accurately in the region.

In addition to modifying the atmospheric attenuation model to support elevation angles below 5°, the algorithm was also updated to allow for user-defined weather parameters to support deterministic atmospheric loss calculations. Custom weather parameters are useful as they enable more accurate attenuation figures, and they have the ability to create vast amounts of training data for neural networks that contain diverse weather parameters. A direct bypass of the atmospheric attenuation calculations was also enabled to allow the user to hardcode a value for the atmospheric attenuation.

3.1 Atmospheric Scintillation Updates

The atmospheric scintillation was updated following the shallow and deep fading processes for elevation angles less than 5° (Ref. 3). The resulting implementation produced a surface as seen in Figure 5. This figure shows how the fade depth (dB) increases at lower elevation angles and at higher frequencies. The scintillation was calculated for typical weather parameters with a probability of exceedance of 2 percent. The discontinuity between the above and below 5° scintillation models is also visible. Note that the transition of the model near elevation angles (θ) of 5° is slightly discontinuous.

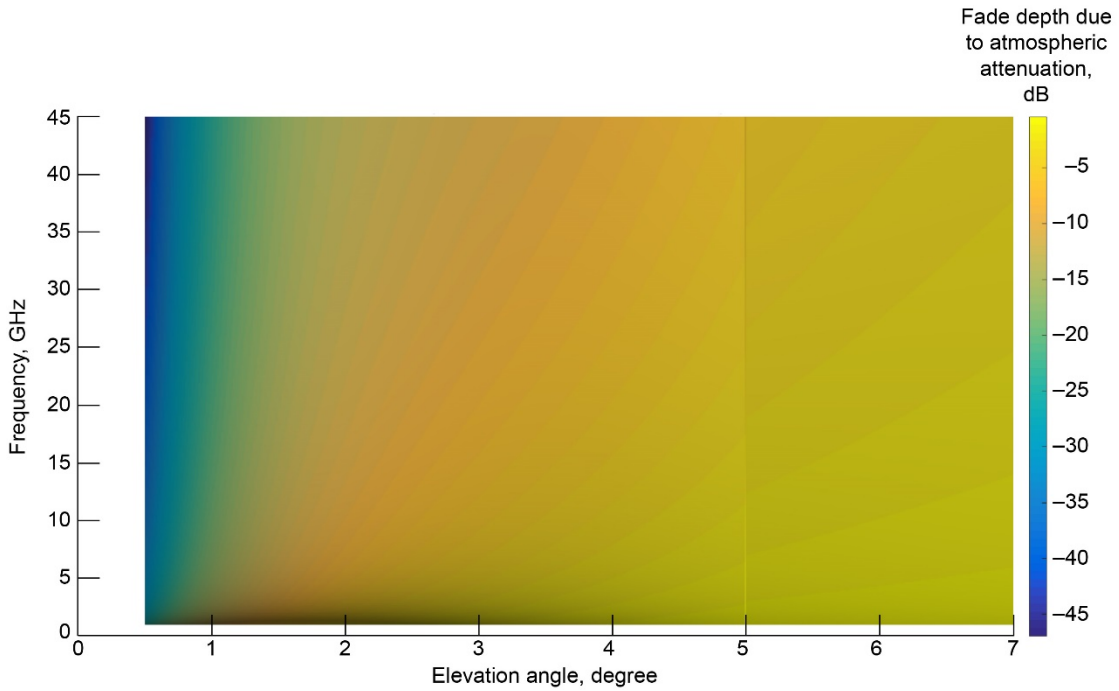

Figure 5.—Scintillation fade depth at low elevation angles.

In the future, an implementation closer to Reference 4 could minimize the discontinuity, although the discontinuity is rather small. Also, θ is not well conditioned near zero. This is because the model from Reference 3 has only been verified to a half a degree. As such, the model is still constrained to a minimum elevation angle of a half-degree.

3.2 Slant Path

The current algorithm estimated slant path distance (D) with a sine function and the height of the atmosphere (H) and transmitting antenna (H_0) from the ground, as seen in Equation (6), when satisfying the inequality in Equation (7), where R_E is the Earth's radius. However, as $\lim_{\theta \to 0} \sin\theta$, the inequality in Equation (7) is no longer satisfied, and thus, this approximation is no longer valid. Therefore, in functions such as the atmospheric rain-rate attenuation function, the sine function is replaced as shown in Equation (8) as provided in Reference 5. Equation (8) makes no approximations, and thus, does not need to satisfy the inequality in Equation (7), giving the correct value for the slant path.

$$D = \frac{\left(H - H_0\right)}{\sin\theta} \tag{6}$$

$$\frac{2\left(H - H_0\right)}{R_E} \ll \sin^2\theta \tag{7}$$

$$\frac{1}{\sin\theta} \to \frac{2}{\left[\sin^2\theta + \frac{2\left(H - H_0\right)}{R_E}\right]^{1/2} + \sin\theta} \tag{8}$$

3.3 Customized Weather Parameters

Communications system analysts that create training data for neural networks desire to have direct control of the calculated atmospheric attenuation based on known weather information at the ground node. To provide more control, an additional change to the atmospheric attenuation model was made, enabling the model to utilize user-provided weather parameters in place of the probabilistic values found from the ground station or vehicle location, time of year, and tabular reference. Figure 6 illustrates a comparative plot of the customized weather versus the probabilistic approach. The difference in attenuation of a configuration using user-provided weather parameters versus tabular reference data is pictured. Since the custom weather parameters in this case were similar to the tabular data parameters, the attenuation curves are similar.

One case where it was not possible to simply use a user-provided value rather than a tabular value pertained to the gaseous loss model portion of atmospheric attenuation calculations. The baseline ITU models (Ref. 6) used tabular references for each of the 922 layers of the atmosphere. It is unreasonable to burden the user with providing 922 separate parameters, so it was decided to transition to a different model. The new model relies solely on the ground conditions to model the gaseous attenuation (Ref. 6). The baseline ITU model used a taxing for loop in order to calculate the attenuation for each of the

922 atmospheric layers. The newer model, however, is vectorized to calculate the attenuation of the various layers, thus optimizing runtime. Figure 7 shows a comparison with the 922-layer ITU model and the new model. The two models are compared over the configurations provided by the ITU. Although the models differ by a fraction of a decibel, they both follow the same trends throughout the configurations.

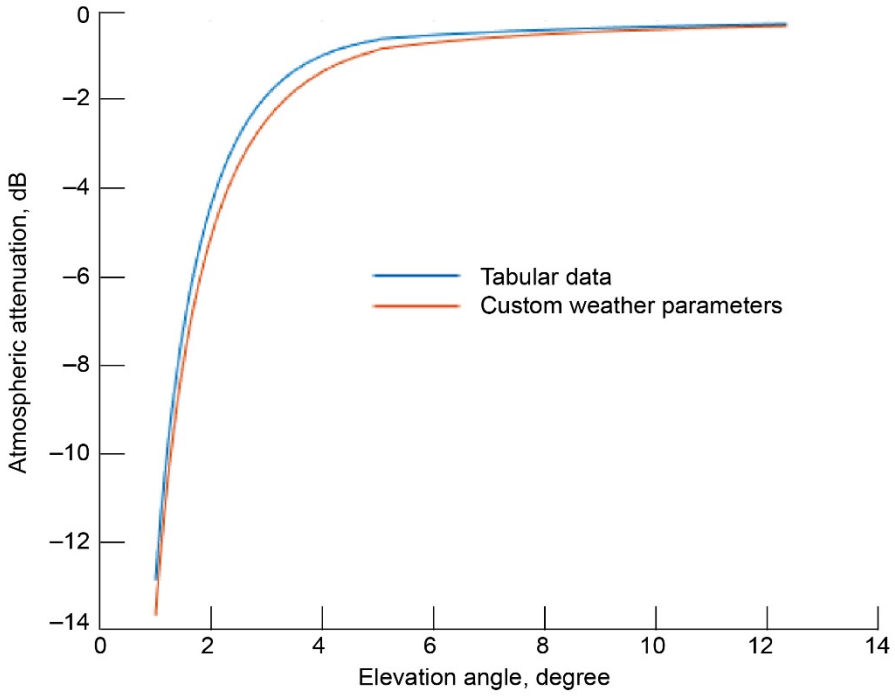

Figure 6.—Atmospheric loss comparison with user-provided weather parameters and tabular data.

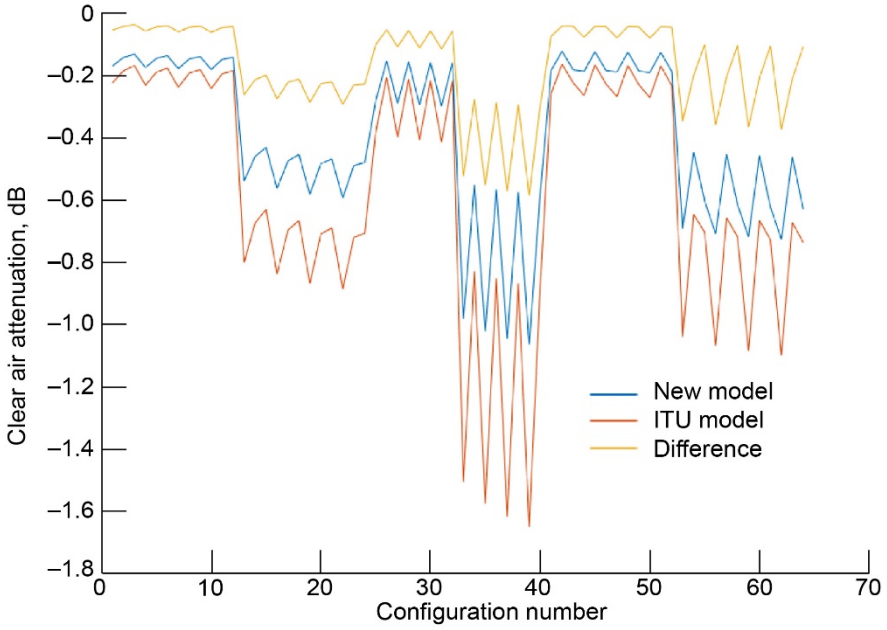

Figure 7.—Comparison of gaseous attenuation models. International Telecommunication Union (ITU).

4.0 Concluding Remarks

The vehicle propagator and atmospheric attenuation updates to the Glenn Research Center's Communication Analysis Suite (GCAS) are important for system analysis in the Artemis Program and other future NASA missions. The vehicle propagator simulates vehicles moving along the surface of planetary bodies. The flexibility of the vehicle propagator allows for many vehicle types, trajectory types, and methods of inputs for the communication performance analysis of vehicles. The flexibility of the vehicle propagator also allows future expansions including terrain mapping, different trajectory types, and various vehicles, such as underwater submarines, can easily be built into the vehicle propagator with few changes.

The atmospheric attenuation model improvements enable higher fidelity communications analysis. The ability to specify weather parameters allows for the higher fidelity analysis and more accurate implementation of the current conditions at the vehicle's location. By changing weather parameters within the analysis suite software, training data with variable weather parameters for neural networks can be generated. The neural networks will learn how the changing weather parameters impact communications, and adapt accordingly.

A second high-fidelity model improvement was added into the GCAS capabilities. The uniform low-elevation updates also improve the accuracy of the capability suite, specifically with respect to vehicle communications links to other vehicles or ground stations. Prior to this update, atmospheric attenuation on vehicles was calculated to a minimum elevation angle of 5°. The update enables communications between vehicles with less than 5° of elevation angle, thus improving the fidelity of analysis possible between vehicles.

Overall, the updates made to the GCAS capabilities improve the fidelity and flexibility of the possible types of analysis use cases. These updates will play an important role in analyzing the communications configuration of future missions, and will provide unique simulation capabilities of future communications technologies such as cognitive communications.

References

1. Williams, Ed: Aviation Formulary. V1.46, 2011.
2. Subirana, J. Sanz; Zornoza, J.M. Juan; and Hernández-Pajares, M.: Transformations Between ECEF and ENU Coordinates. Technical University of Catalonia, Spain, 2011. http://www.navipedia.net/index.php/Transformations_between_ECEF_and_ENU_coordinates Accessed Aug. 1, 2019.
3. International Telecommunications Union: Propagation Data and Prediction Methods Required for the Design of Earth-Space Telecommunication Systems. Recommendation ITU–R 618–13, 2017.
4. Lee, Charles H.; Cheung, Kar-Ming; and Ho, Christian: A Unified Low Elevation Angle Scintillation Model. Presented at the 2011 IEEE International Symposium on Antennas and Propagation, Spokane, WA, 2011, pp. 821–824.
5. Manning, Robert M.: A Rain Attenuation Model for Satellite Link Attenuation Predictions Incorporating the Spatial Inhomogeneity of Rainrate. Int. J. Sat. Comm., vol. 2, no. 3, 1984, pp. 187–197.
6. Rogers, D.: Propagation Considerations for Satellite Broadcasting at Frequencies Above 10 GHz. IEEE J. Sel. Area Comm., vol. 3, no. 1, 1985, pp. 100–110.

Bibliography

Clynch, James R.: Geodetic Coordinate Conversions. I. Geodetic to/from Geocentric Latitude. 2006. http://clynchg3c.com/Technote/geodesy/coordcvt.pdf Accessed Aug. 8, 2019.

International Telecommunication Union: Attenuation by Atmospheric Gases. Recommendation ITU–R P. 676–10, 2013.